Journal of
Ceramic Science
and Technology

J. Ceram. Sci. Tech., **03** [01] 17-28 (2012)
DOI: 10.4416/JCST2012-00040
available online at: http://www.ceramic-science.com

Thermodynamic, Equilibrium, and Kinetic Studies of Adsorption of Pillarized and Organofunctionalized Smectite Clay for Th^{4+} Removal

D.J.L. Guerra*[1], E.S. Menonça[1], R.A.R. Silva[1], W. Lara[1]

[1]Department of Mineral Resources, Federal University of Mato Grosso, DRM-ICET-UFMT, Cuiabá, Mato Grosso, Brazil 78060 900.

received November 1, 2011; received in revised form November 28, 2011; accepted January 18, 2012

Abstract

A natural smectite clay sample was taken from the Amazon region, Amazonas State, Brazil. Zirconium polyoxycations were inserted into the smectite structure in a pillaring process. The pillarized smectite was organofunctionalized with the compound 3-mercaptopropyltrimethoxysilane. The natural and modified clay samples were used for the adsorption of tetravalent thorium cation from aqueous solution in a batch process. The adsorption process was fitted to equilibrium and kinetic models. The effects of stirring time, adsorbent dosage and pH on the adsorption capacity demonstrated that 90 min is sufficient to reach equilibrium at room temperature at pH 6.0. From the cation/basic center interactions for each smectite at the solid-liquid interface, the equilibrium constant and exothermic thermal effects were calculated with calorimetric methodology. By considering the net interactive number of moles for thorium cation and the equilibrium constant, the enthalpy, ΔH^0_{int} (-7.2 ± 0.11 to -7.0 ± 0.11 kJ mol^{-1}) and negative Gibbs free energy, ΔG^0_{int} (-22.4 ± 0.1 to -23.1 ± 0.1 kJ mol^{-1}) were calculated. These values enabled determination of the positive entropy, ΔS^0_{int} (51.2 ± 0.1 to 54.1 ± 0.1 JK^{-1}mol^{-1}). All liquid/solid interface adsorptions were spontaneous in nature and enthalpically driven.

Keywords: Smectite, adsorption isotherms, thorium, thermodynamic, kinetic

I. Introduction

Industrial activities generate a wide diversity of wastewaters, often containing agents that cause pollution, which can result in dangerous consequences for human beings owing to their effect on ecosystems. To minimize these unfavorable conditions, adsorption methodologies have been proposed as an alternative process for resolving such problems. In this context, many materials have been proposed and some of them are useful candidates, such as natural and functionalized clay surfaces [1,2]. Organoclay produced from synthetic clay has also been studied for various applications. These included (i) the preparation of modified electrodes for electrochemical application and biosensors [3], (ii) the immobilization of several enzymes [4], (iii) the preparation of hybrid compounds [5], (iv) the immobilization of antifungal compound [6], and (v) the preparation of polymer/clay nanocomposites [7].

Taking into account pristine smectite chemical composition with original acidic or basic active functions, useful for surface chemical modification, through inclusion of some other active groups, then, the possibility of application is significantly increased, including those related to cation removal from waters, simulating also wastewater effluents [8,9]. For this purpose thorium was chosen for the present investigation owing to the fact that this metal can be discharged to the environment, originating, for example, from paint production,pharmaceutical and industrial chemical processes and may cause damage to soil, aquatic media, fauna, and flora [10]. To eliminate this undesirable poison from an ecosystem, several methods have been proposed, such as electrodeposition, solvent extraction, membrane and separation, adsorption on activated or/and chemically modified clays [11].

Activated carbon was widely employed as the common adsorbent for effluent treatment. Activated carbon requires the utilization of chelating agents for the removal of pollutant species, making this procedure even more expensive. Phyllosilicates and zeolites play a prominent role in nuclear-waste processing and in its management, as they are well known for their stability at high temperature and in radiation fields [12 – 15]. Meeting the stringent coolant-purity requirements of the nuclear industry is solely attributable to inorganic ion exchangers. In recent years, clays, layered materials, and zeolites have been used extensively in the chemical decontamination process for radionuclide recovery, regeneration of decontaminants, and removal of the formulation chemicals from the coolant [16 - 18]. The chemical modification process has been used for optimization of the physical-chemical properties of clay minerals. A pillaring material may be prepared generally by using inorganic pillars, such as aluminum, zirconium, and iron. The intercalated inorganic molecules act as pillars that hold the 2:1 layers of smectite permanently apart. An organophillic material may be prepared by means of the intercalation of silylant agents, like

* Corresponding author: denis@cpd.ufmt.br

the compound 3-mercaptopropyltrimethoxysilane. These hybrid materials were called organoclays (generic name for phyllosilicates that have been organofunctionalized), organosmectite or organomontmorillonite (designation for montmorillonite group when the minerals that make up this group are used as raw material) [19 - 21]. Organoclays display distinct adsorptive and sorptive properties depending on the molecular sizes of the alkyl groups. In this study the reactive group consists of sulfur atoms anchored in a pendant chain.

The aim of the present investigation is focused on the retention capacities and thermal effects of a smectite obtained from the Amazon region. The natural and chemical aspects related to the chemical modification of the clay structure are presented. The chemical modification was effected in two steps. First, the natural smectite was pillarized with zirconium polyoxycations and second organofunctionalized with the silylant agent 3-mercaptopropyltrimethoxysilane. The natural clay and new hybrid phyllosilicate were able to remove Th^{4+} from aqueous medium; based on error function values, the data were best fitted to the Langmuir, Freundlich, and Sips isotherm models. The performance in adsorbing Th^{4+} cation from natural water under dynamic flow (column) conditions was also studied and the results confirmed the batch experiments. The energetic effect caused by the tetravalent cation/sulfur basic center on smectite interactions at the solid/liquid interface was determined with the calorimetric titration procedure.

II. Experimental

(1) Raw material and reagents

The clay was sampled in the Amazon region, in northern Brazil. The natural smectite sample, named SMC-1, with smaller than 2.0 µm particles, was separated by means of sedimentation. The cation-exchange capacity (CEC) was measured in order to evaluate the potential use of clay for intercalation, in accordance with the ammonium acetate method with concentrations of 2.0 mol dm^{-3} at pH 8.0. The cation-exchange capacity is expressed in terms of milliequivalents per 100 g of clay and is written as meq/100 g. The result obtained was 148.0 meq/100 g (SMC-1) on an air-dried basis. Chemical characterization was also performed, using analytical techniques that will be described below. The natural phyllosilicate sample was activated in a stream of dry nitrogen by heating at 423 ± 1 K for 10 h and used immediately.

Reagent-grade solvents were used. 3-mercaptopropyltrimethoxysilane (Fluka) $HS(CH_2)_3Si(OCH_3)_3$ (≥ 97.0 %, 1.057 g cm^{-1} at 398 ± 1 K) was used. Other chemicals such as methanol and ethanol were of reagent grade. Stock standard solution 5000.0 mg L^{-1} of Th^{4+}, which was obtained from primary-standard $Th(NO_3)_4H_2O$ (Aldrich) with a concentration of 0.050 mol dm^{-3}, was used as the cation source, and it was added in increments of 10.0 mm^3 [22, 23]. Doubly distilled deionized water (DDW) was used for the preparation of solutions, wherever required. Solutions of thorium were prepared from suitable serial dilution of the stock solution in DDW.

(2) Sample preparation

The natural clay sample was ground and sieved through a USS (200-mesh) 0.074-mm sieve, dried in an oven at 333 ± 1 K to reach humidity between 12 and 15 %, as monitored with the thermogravimetric technique (TGA). A preliminary X-ray powder diffractometry analysis was used to confirm the presence of the smectite clay fraction through conventional procedures: air-dried, ethylene glycol solvated, and heated at 573 and 773 ± 1 K [1].

(3) Chemical modification

For the pillaring process, a stock solution of zirconium (0.10 mol dm^{-3}) was prepared for use as pillaring solution, $ZrOCl_28H_2O$ (Aldrich) was used as the zirconium source. Approximately 5 g natural smectite (SMC-1) was suspended in 100.0 cm^3 of the zirconium pillaring solution at room temperature under vigorous stirring for 25 h. The resulting suspension was centrifuged at 4000 rpm for 60 min. The liquid was decanted to prevent the finer particles from re-entering suspensions and the solid was dried at 323 ± 1 K for 17 h, to produce the sample named $SMC\text{-}1_{Zr}$ [24].

A mass of approximately 5 g pillared smectite sample ($SMC\text{-}1_{Zr}$) was suspended with 5.0 cm^3 of the silylating agent 3-mercaptopropyltrimethoxysilane in xylene under reflux in an inert nitrogen atmosphere and with mechanical stirring for 3 h. The solution was filtered through sintered glass and the solid was dried under vacuum for 12 h, to give the respective $SMC\text{-}1_{Zr/SH}$ matrix.

(4) Adsorption

Firstly, the effect of pH on adsorption for two clay samples was evaluated by varying this parameter over the range from 1.0 to 11.0, with addition of 0.10 mol dm^{-3} nitric acid or sodium hydroxide. The pH of the solutions was measured with a pH/Ion, model 450 M, Analyzer, SP, Brazil.

The adsorption experiments were conducted according to the batchwise method by suspending a series of 20.0-mg samples of two clay types in 20.0 cm^3 aqueous solutions of metal at concentrations varying from 0.125 to 3.50 x 10^{-5} mol dm^{-3}, under orbital stirring for 24 h at 298 ± 1 K [22, 24]. The centrifugation was used for solid separation of metallic solution. Samples were carefully pipetted from the supernatant of metallic solution for determination of Th^{4+} concentrations. The metallic ion final concentrations were determined with a Perkin Elmer Flame Atomic Absorption Spectrometer model Analyst 200 using an air-acetylene flame. A hollow cathode lamp of thorium ($\lambda_{Th(IV)}$=232.038 nm) from the same manufacturer was used as the radiation source. The Th^{4+} adsorption capacities (N_f) of the phyllosilicates were calculated as follows (Eq. (1)), for series of isotherms, it was revealed that the adsorption process conforms to the equilibrium models. The isotherm equations corresponding to the Langmuir [25], Freundlich [26], and Sips [27] models are presented in Table 1. The kinetic equations corresponding to the Avrami, pseudo-first-order, and pseudo-second-order models [28] are given in Table 1.

$$N_f = \frac{N_i - N_e}{m} \quad (1)$$

where N_i is the initial number of moles of thorium added to the system, N_e is the amount remaining after the equilibrium and m is the mass in grams of the adsorbent. Profiles of the obtained adsorption isotherms were represented by the number of moles per gram adsorbed (N_f), versus the number of moles at equilibrium per volume of solution (C_S).

Table 1: Isotherms equilibrium and kinetic adsorption models

Adsorption models	Nonlinear equations
Isotherms equilibrium models	
Langmuir	$N_f = \frac{N_L K_L C_S}{1 + K_L C_S}$
Freundlich	$N_f = K_F \cdot F_S^{\frac{1}{n_F}}$
Sips	$N_f = \frac{N_L K_S C_S^{\frac{1}{n_S}}}{1 + K_S C_S^{\frac{1}{n_S}}}$
Kinetic models	
Avrami	$N_t = N_E \left[1\text{-}\exp\left[-\left(k_{AV}t\right)\right]^{n_{AV}}\right]$
Pseudo-first-order	$N_t = -N_E \left[1 - \exp\left(-k_f t\right)\right]$
Pseudo-second-order	$N_t = \frac{N_E^2 k_s t}{1 + k_S N E t}$

An aliquot of 1.0 g of each smectite sample was added into a glass column measuring 200.0 mm in length and 10.0 mm in diameter, forming a section of column that was used in the dynamic flow. To determine the effect of concentrations of Th^{4+} and flow rates on the column adsorption, two concentrations of thorium solution (0.10 and 0.30 mg dm^{-3}) and flow rates, 5.0 and 10.0 cm^3 min^{-1}, were defined. The effluent solutions were collected, and every 10 cm^3 was selected as a sample to determine the concentration of radionuclide in the effluent solutions and thorium ion contents were determined using flame atomic absorption spectrometry (Analyst 200, Perkin-Elmer). The column adsorption capacity (N_{ed}) was calculated with Eq. (2) expressed as [29]:

$$N_{ed} = \frac{(C_0 V_0 - \Sigma C_n V_n)}{m} \quad (2)$$

where N_{ed} is the amount of Th^{4+} adsorption per gram SMC-1 or SMC-$1_{Zr/SH}$ at saturation (mg g^{-1}), C_0 is the original concentration of thorium (mg dm^{-3}), V_0 is the volume of the effluent solution (dm^3), C_n is the concentration of sample n (mg dm^{-3}), V_n is the volume of sample n (dm^3), and m (g) is the amount of smectite clay samples.

The thermal effects from metal cation interacting on natural and modified smectite samples were observed by means of calorimetric titration with an isothermal calorimeter, Model LKB 2277, from Thermometric. In this titration, the metallic solution is added to a suspension of about 20 mg of the phyllosilicate sample in 2.0 cm^3 of water, under stirring at 298 ± 1 K. A series of increments of 10 x 10^{-6} dm^3 of metal solutions was added to the metal-phyllosilicate to obtain the thermal effect of interaction (Q_t). Two other titrations are needed to complete the full experiment: (i) the thermal effect due to hydration of the phyllosilicate sample (Q_h), which normally gives a null value and (ii) the dilution effect of metal solution in water, without any sample in the vessel (Q_d). The resulting thermal effect is given by following Eq. (3) [30 - 40].

$$\Sigma Q_r = \Sigma Q_t - \Sigma Q_d - \Sigma Q_h \quad (3)$$

(5) Analytical procedures

The natural SMC-1 clay sample was analyzed with Inductively Coupled Plasma-Optical Emission Spectrometry (ICP-OES), using an ARL 34000 instrument. The over-dried powdered sample weighing approximately 225 mg, was placed on weighed glass dishes and transferred quantitatively to pre-cleaned nitric and digestion bottles. The sample was then digested with 5.0 cm^3 concentrated nitric and hydrochloric acids in 1:3 proportions in volume, with an identical volume of hydrofluoric acid over five days. The SMC-1 was cooled in an ice-bath and 20.0 cm^3 of 0.10 mol dm^{-3} boric acid was added under stirring, followed by 50.0 cm^3 of DDW, and the solution was then diluted to 100.0 cm^3. For each sample, a blank and a set of elemental standards were run to calibrate the instrument.

For infrared spectroscopy, the samples were oven-dried at 393 ± 1 K to remove any adsorbed water. Each sample of about 1.3 mg was finely ground for 1 min, combined with 100 mg of oven-dried spectroscopic grade KBr and pressed with 7.0 t into a disc under vacuum. The spectrum of each sample was recorded in triplicate between 1250 to 4000 cm^{-1} by accumulating 64 scans at 4 cm^{-1} resolution, using a Perkin-Elmer 1760X Fourier transform infrared spectrometer.

Carbon, nitrogen, and hydrogen contents were determined on a Perkin-Elmer 2400 Series II microelemental analyzer. At least two independent determinations were performed for each clay sample.

Thermogravimetric curves were obtained from approximately 10 mg smectites on the Thermogravimetric analyzer model TA-2960 in a dynamic atmosphere using dry nitrogen flux, with heating from room temperature up to 1050 ± 1 K at a heating rate of 288 ± 1 K min^{-1}, kinetic thermal parameters were calculated from the Coats-Redfern equation [41].

Brunauer-Emmett-Teller (BET) surface area, pore diameter and pore volume were obtained from nitrogen adsorption/desorption in a Micromeritics ASAP 2000 BET surface analyzer system. The mesopore size distribution was obtained by applying the Barret-Joyner-Halenda (BJH) method to the adsorption branch of the isotherm.

III. Results and Discussion

(1) Characterization of smectite samples

The elemental analysis of the natural sample SMC-1 gave results consistent with smectite as principal clay mineral and quartz clay mineral presence, with silicon, aluminum, and iron being the major elemental quantities contained in the well-organized structure, by presenting the chemical composition 58.3, 16.8, 6.5, 4.2, 0.2, 2.3, and 1.7 % of SiO_2, Al_2O_3, Fe_2O_3, MgO, Na_2O, CaO, and K_2O, respectively,

and 10.0 % in mass was lost in the ignition process. Thus, the composition of this natural smectite, calculated from the chemical analysis, gives the formula (Eq. (4)):

$$(Na_{0.02}K_{0.16}Ca_{0.17})(Al_{1.25}Mg_{0.42}Fe_{0.32})(Si_{3.89}Al_{0.11}O_{10})(OH)_2 \quad (4)$$

The successful immobilization was clearly expressed in the elemental analyses of the chemically immobilized surface. The values for carbon, hydrogen, and nitrogen were obtained from CHN analyses, of: 14.31 ± 0.12 %, 3.43 ± 0.10 %, and 8.31 ± 0.10 %, respectively. The degree of organofunctionalization was calculated based on the amount of nitrogen and carbon atoms on the chemically modified smectite samples. Based on the analytical data for the nanocompound, the density of these pendant organic molecules immobilized on smectite layers can be calculated. Thus, the silylating agents grafted onto smectite structure gave an amount of 9.2 ± 0.11 mmol g^{-1} for SMC-$1_{Zr/SH}$.

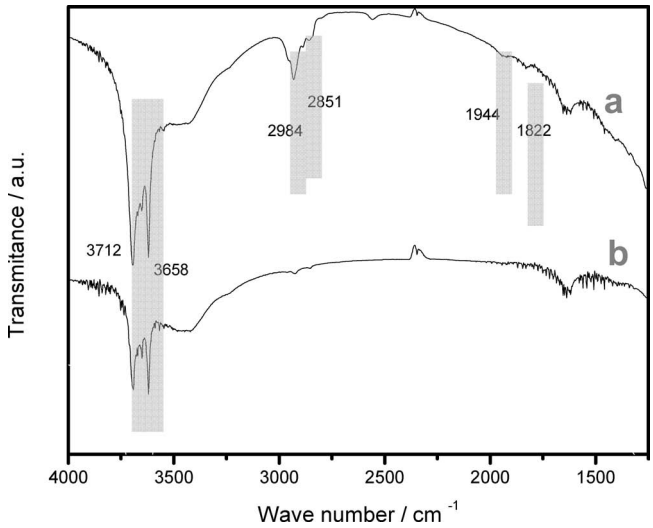

Fig. 1: FTIR spectra of the smectite samples: SMC-$1_{Zr/SH}$ (a) and SMC-1 (b).

The infrared spectra for natural and chemically modified smectites showed broad bands at 3658 and 3712 cm^{-1} (Figs. 1a and 1b), attributed to the O-H group, which could be bonded to silicon, iron or aluminum atoms on the inorganic backbone [30]. Such hydroxyl groups can be sited at the corners and fractures of sheets or are formed by tetrahedral inversion processes. The new low band at 2984 cm^{-1} probably appeared due to the existence of C-H vibration of the remaining methoxy groups or from CH_2 groups of the chain of the silylating agent, which indicates the successful preparation of the chemically anchored surface [31]. A weak band at 2851 cm^{-1} was observed in the modified matrix spectrum, which was attributed to the O-CH_3 group. Moreover, bands at 1944 and 1822 cm^{-1}, related S-H stretching vibration are observed for the anchored surfaces, corroborating again with the immobilization process, as shown in Fig. 1a.

Thermogravimetric curves for SMC-1 and SMC-$1_{Zr/SH}$ are present in Figs. 2a and 2b, respectively. The samples showed two characteristic decomposition stages: one starting at 300 – 450 K, assigned to water loss, this decomposition was observed in both smectite types and another mass loss between 800 – 1050 K (SMC-$1_{Zr/SH}$), assigned to the decomposition of the organic pendant groups onto natural smectite and water loss during the condensation silanol siloxane groups [42, 43].

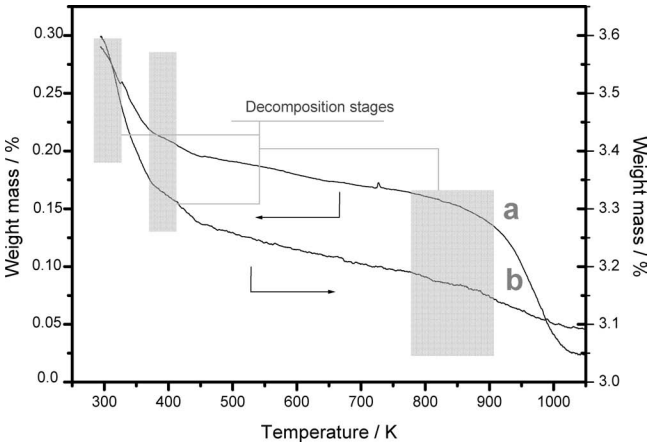

Fig. 2 : Thermogravimetric curves of smectite samples: SMC-$1_{Zr/SH}$ (a) and SMC-1 (b).

The TG curves data were used to explore the mechanism of the individual stage. The well-characterized decomposition stages of SMC-1 and SMC-$1_{Zr/SH}$ matrices were selected for study of the kinetic decomposition. The kinetic parameters, activation energy (E_a) and pre-exponential factor (A), were calculated using the Coats-Redfern Eq. (5) [44].

$$\log\left[\frac{1-(1-\alpha)^{1-n}}{T^2(1-n)}\right] = \log\left[\frac{AR}{\varphi E_a}\left(\frac{2RT}{E_a}\right)\right] - \frac{E_a}{2.303RT} \quad (5)$$

where α is a fraction of weight loss, n is the order of reaction, T (K) is the temperature, A is the pre-exponential factor, R is the gas constant (8.314x10^{-3} kJ K^{-1} mol^{-1}), φ is the heating rate, and E_a is the activation energy. The order of reaction (*n*) is the one for which a plot of the Coats-Redfern expression gives the best straight line among various trial values of *n* that are examined relative to that estimated with the Horovitz-Metzger model [45]. A plot of $\log\left[\frac{1-(1-\alpha)^{1-n}}{T^2(1-n)}\right]$ versus $\frac{1}{T}$ gives the slope from which activation energy (E_a) was determined. Thus, the activation energy and pre-exponential factor entropic values for SMC-1 and SMC-$1_{Zr/SH}$ were 29.21 and 36.90 kJmol^{-1} and 1.18 x10^9 and 2.61 x 10^9, respectively, kinetic thermal analysis shows that the E_a and A values decrease in the order SMC-$1_{Zr/SH}$ > SMC-1. Indeed, this behavior must be due to the fact that modified smectite samples have a lower surface area than natural smectite, resulting in a more difficult decomposition of the pendant group attached to the smectite surface.

The BET surface areas of the natural and modified phyllosilicate samples demonstrated that chemical modification caused the formation of pore surface in the solid particles, resulting in a higher surface area, revealing 459.8 m^2 g^{-1} for SMC-$1_{Zr/SH}$ 358.9 for SMC-1_{Zr} and relative to the natural SMC-1 sample with 51.8 m^2 g^{-1}. The pore diameters change in the same direction, varying from 1.2 nm for the natural phyllosilicate to 4.6 nm for the pillared silicate and 5.2 nm for the anchored and pillared silicate. The results of this textural analysis indicate that the materials should be alternatives for metallic ion removal.

Table 2: Adsorption and thermodynamic data for Th^{4+} adsorption for unmodified and modified smectite samples (clay 1.0 g dm^{-3}, pH 6.0, time 150 min at 298 ± 1 K)

Sample	N_f^{max} (mmol g^{-1})	$K_L x10^{-3}$ (dm^3 $mmol^{-1}$)	R^2	N_s (mmol g^{-1})	$-\Delta h^0_{int}$ (Jg^{-1})	$-\Delta H^o_{int}$ ($kJmol^{-1}$)	LnK_L	$-\Delta G^o_{int}$ ($kJmol^{-1}$)	ΔS^o_{int} ($JK^{-1}mol^{-1}$)
SMC-1	1.55± 0.12	1.173± 0.13	0.997	1.5± 0.12	11.2± 0.13	7.2 ± 0.01	9.12	22.4 ± 0.1	51.2 ± 0.1
$SMC\text{-}1_{Zr/SH}$	1.89± 0.11	1.248± 0.12	0.989	1.8± 0.13	12.4± 0.14	7.0 ± 0.11	9.31	23.1 ± 0.1	54.1 ± 0.1

(2) Adsorption and thermodynamic study

The batch adsorption experiment can provide information about the amount adsorbed at equilibrium, information that cannot be gained from steady state measurements. In this context, the Th^{4+} ions were examined within a range of pH 1.0 -11.0. Fig. 3a shows the influence of pH on the adsorption process of Th^{4+} onto natural and modified smectite types. The data reveals maximum values of N_f^{max} around pH 6.0 for two clay samples. As can be seen from Fig. 3a, the adsorption of Th^{4+} on natural and modified smectite samples mainly occurs at $5.0 < pH < 7.0$. The adsorption of Th^{4+} increases substantially at $pH < 6.0$. Results emphasize that with an increase in the pH of the solution, the N_f^{max} adsorbed increases for two systems. Therefore the efficiency of Th^{4+} on unmodified and modified phyllosilicates can be controlled by the initial pH of the solid/liquid reaction. The reason for the low adsorption capacity in a high pH is the competition between the excess of OH^- species in the medium [46, 47]. Also, higher acid concentrations suppress hydrolysis of the Th^{4+} ions. In addition, the adsorption of Th^{4+} on smectite types is mainly dominated by ion-exchange or outer-sphere complexation at low pH values, and by inner-sphere complexation at high pH [48, 49]. Consequently, the number of moles of Th^{4+} removal may decrease at a low pH.

The adsorption of thorium cation on unmodified smectite and its chemically modified forms are shown in Fig. 3b. The influence of the incorporated molecules on the smectite structure and on the mutation of adsorption capacity was observed based on saturation adsorption values, as represented by the respective isotherms. The results of applying equilibrium adsorption models for unmodified smectite and its modified forms are listed in Table 2. The Langmuir adsorption model can be used to explain the significant capacity of the chemically modified smectite to quantify thorium cation interaction. The Langmuir model presents a significant advantage in comparing the experimental data; it allows quantification of the capacity of retaining cations within the structure of the matrix and evaluation of the constant related to the bonding energy.

The interaction of cations with immobilized external and internal surfaces of the smectite structure is governed by the microenvironment around each arrangement, which is usually composed of reactive basic centers, mainly in the internal hydrated structure. Such hydroxyl groups act as bridgings that favor the smectite matrix intercalation process. This process gives the pendant anchored chains with available amino groups inside the interlayer space, available to bond to appropriate cations, such as Th^{4+}.

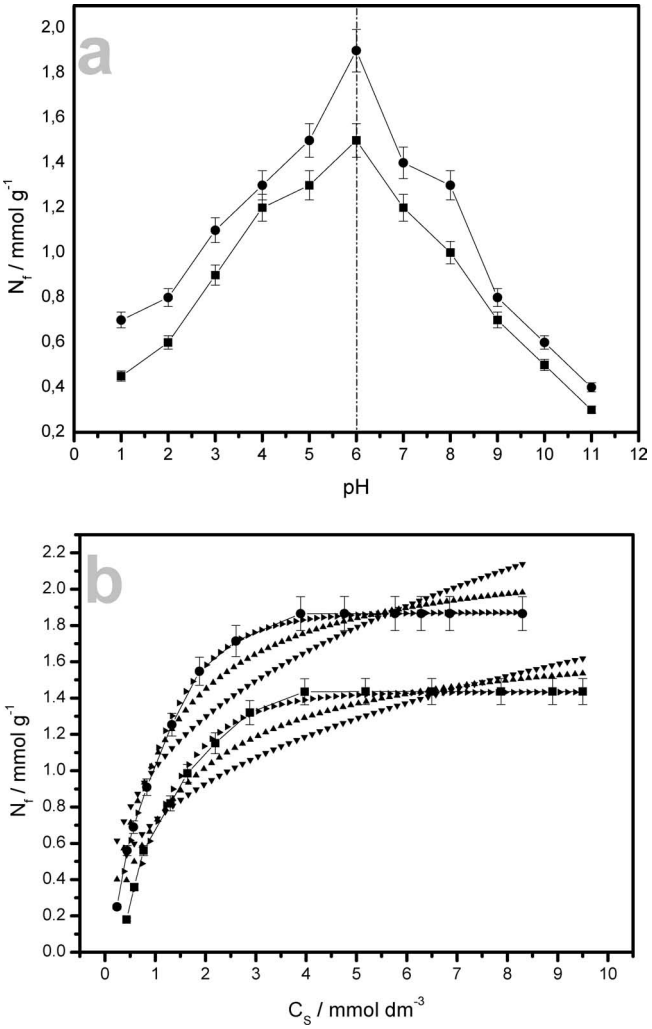

Fig. 3 : Effect of pH on Th^{4+} adsorption (a) and effect of concentration of Th^{4+} adsorption (b) onto smectite samples: SMC-1 ■ and $SMC\text{-}1_{Zr/SH}$ • and isotherms calculated with non-linear method: Sips ▲, Langmuir ▶, and Freundlich ▼ at pH 6.0, after 150 min at 298 ± 1 K.

From the adsorption isotherm for thorium cation, represented by a C_s versus N_f plot, the calculated curves were obtained with the non-linear method, as shown in Fig. 3 b, whose data were adjusted to the Langmuir, Freundlich, and Sips isotherm models, as before. For a series of calorimetric titrations, the number of increments and the volumes of thorium cation needed to saturate the mass of the smectite samples [39] are listed in Table 2. The adsorption process was evaluated from the results obtained, by considering the adsorption isotherms and the molar fraction of the thorium cation in solution. The experimental data were better adjusted to a Langmuir model ($R^2 \sim 0.99$), in which it is assumed that monolayer of thorium cations is formed on the chemically modified smectite surface. For

this model the results obtained were adjusted to Eq. (2). The maximum adsorption capacities, N_f^{max}, for thorium onto unmodified and modified smectite are listed in Table 2, which shows that the values are highest for the chemically modified smectites. This behavior is attributed to the optimization of the physical chemical properties, consequently, to the larger surface capacity to bond species.

The molar fraction of the thorium cation in the supernatant in equilibrium for each point of the calorimetric titration (X) was calculated by considering the number of moles of the solute (N_s) and the number of moles of water (N_{wat}) [39].

$$X = \frac{N_S}{(N_S + N_{wat})} \quad (6)$$

The calculated X values and the data obtained from calorimetry were adjusted to the modified Langmuir model [38] expressed by Eq. (6). The calorimetric results are presented in Fig. 4 and listed in Table 2.

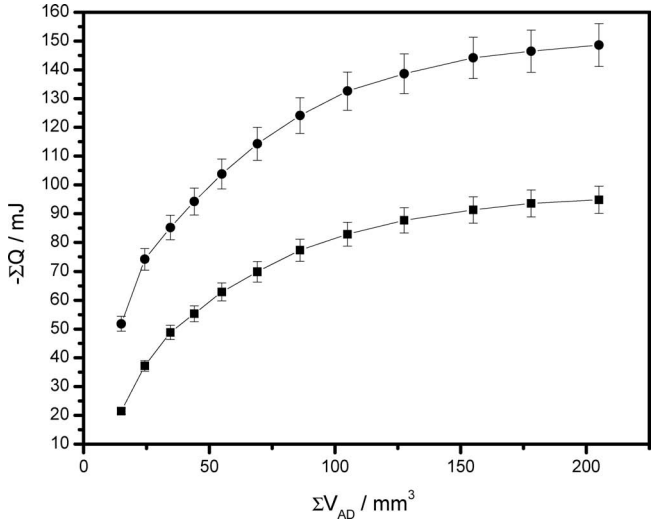

Fig. 4 : Isotherms of thermal effects for thorium adsorption for SMC-1 ■, and for chemically modified smectites SMC-$1_{Zr/SH}$ • at pH 6.0, after 150 min at 298 ± 1 K.

$$\frac{\Sigma X}{\Sigma \Delta h_r^0} = \frac{1}{(K_L + 1)\Delta h_{int}^0} + \frac{\Sigma X}{\Delta h_{int}^0} \quad (7)$$

where $\Sigma \Delta h_r^0$ is the thermal effect of thorium-SMC-1/SMC-$1_{Zr/SH}$ surface interactions, Δh_{int}^0 is the thermal effect of formation of the thorium monolayer on the modified smectite surface, the analysis of the energetic of systems is based on the Langmuir theory, which is a theory for monolayer molecular adsorption, and K_L is a proportionality constant that also includes the equilibrium constant.

The isotherm data obtained from the calorimetric titrations were used in a $\Sigma \Delta h_r^0$ versus ΣX plot and the linearized form is given by a $\frac{\Sigma X}{\Sigma \Delta h_r^0}$ versus ΣX plot [31]. From the enthalpy of formation of monolayer Δh_{int}^0 and the number of moles of thorium, N_s, adsorbed on the modified smectite matrix, the enthalpies of interaction can be calculated with Eqs. (8) and (9):

$$\Delta H_{int}^0 = \frac{\Delta h_{int}^0}{N_S} \quad (8)$$

$$\beta = \frac{1}{\Delta h_{int}^0} \quad (9)$$

where β is the angular coefficient obtained from Eq. (8). Taking these values into account (Eq. (10)):

$$\Delta G_{int}^0 = RT\ln K_L \quad (10)$$

where K_L is the equilibrium constant obtained from the Langmuir model, T is the absolute temperature, the universal gas constant R = 8.314 x 10^{-3} kJ K^{-1} mol^{-1}. Eq. (11) relates the energies involved.

$$\Delta G_{int}^0 = \Delta H_{int}^0 - T\Delta S_{int}^0 \quad (11)$$

The thermodynamic cycles for this series of intercalations involving a suspension (susp) of smectite matrices (SMC-1_X) in aqueous (aq) solution with thorium cation (M^{4+}) can be represented by the following calorimetric reactions (Eqs. (12 – 15)):

$$SMC\text{-}1_{X(susp)} + M^{4+}(aq) = SMC\text{-}1_X \cdot M^{4+}_{(susp)}, \quad Q_t \quad (12)$$

$$SMC\text{-}1_{X(susp)} + nH_2O = SMC\text{-}1_X \cdot nH_2O_{(susp)}, \quad Q_h \quad (13)$$

$$M^{4+}_{(aq)} + nH_2O = M^{4+} \cdot nH_2O_{(aq)}, \quad Q_d \quad (14)$$

$$SMC\text{-}1_{X(susp)} + M^{4+}_{(aq)} = SMC\text{-}1_X \cdot M^{4+}_{(susp)} \quad Q_r \quad (15)$$

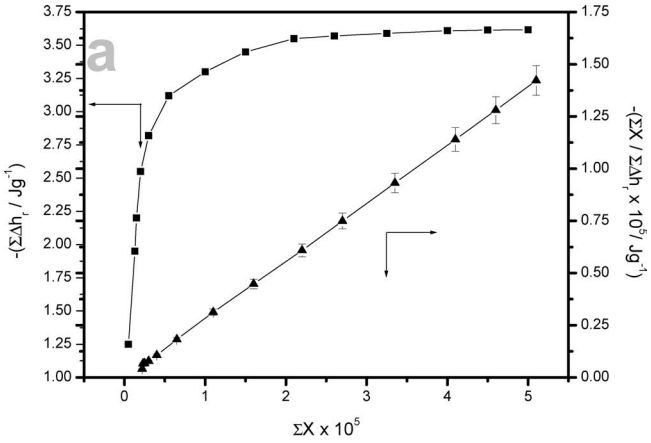

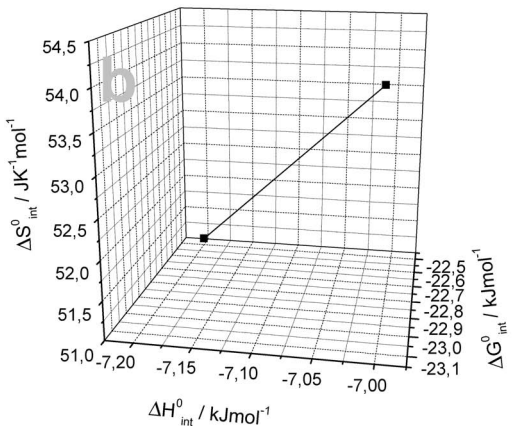

Fig. 5 : Isotherm for calorimetric titration of about 10 mg of chemically modified smectites SMC-$1_{Zr/SH}$ ■ suspended in 2.0 cm^3 of 5.0x10^{-2} mol dm^{-3} at 298 ± 1 K. The straight line is the isotherm in linearized form ▲ (a) and relationship of thermodynamics adsorption values ■ (b) at pH 6.0, after 150 min at 298 ± 1 K.

As the thermal effect of the smectite hydration is null, then the net thermal effect for the complete calorimet-

ric titration is given by $\Sigma Q_r = \Sigma Q_t - \Sigma Q_d$, as represented by Eq. (15), and shown by the experimental data of the isotherms in Fig. 4. From the equilibrium constant, the Gibbs free energy was calculated from Eq. (10) and combined with the enthalpic value, the entropy can also be calculated with Eq. (11). One example of linearization involving thorium cation adsorption is shown in Fig. 5a, from which the angular and linear coefficients could also be obtained. After adjusting the data to the modified Langmuir equation, the resulting values were applied to find Δh^0_{int} values that are the thermal effect of the monolayer. From these data the values of constant K_L can be calculated. The relationship between thermodynamics values adsorption for two systems is presented in Fig. 5b. A résumé of the thermodynamic values obtained in the present study involving thorium cation with modified smectite samples is given in Table 2 and Fig. 5b, showing exothermic enthalpic effects resulting from the chemical modification process. In all cases, the Gibbs free energy for the chemically modified smectite samples demonstrated that the interaction of thorium cation with the modified smectite samples occurred in a spontaneous way. The entropic values were practically constant, suggesting that a similar behavior occurred in the system, during bond formation. The missing thermodynamic data, the entropy values are also listed in Table 2. These values suggest that, during complex formation, the desolvation disturbs the structure of the reaction medium to promote the disorganization of the system and, consequently, leads to an increase in entropy [37]. The highest entropic values have been observed for cations with the largest hydration volumes and illustrate the principle that the loss of water of hydration leads to a disorganization of the final systems [33]. In conclusion, all thermodynamic values are favorable, with exothermic enthalpy, negative free Gibbs energy and positive entropy, data corroboration exists with thorium cation/SMC-1/SMC-$1_{Zr/SH}$ interaction at the solid/liquid interface.

(3) Kinetic adsorption

Investigations of sorption kinetics processes are an important aspect to be considered in aqueous medium treatment as they provide valuable data about the mechanism of sorption process. The adsorption data for thorium uptake versus contact time for a fixed adsorbent amount is presented in Fig. 6a, giving identical abrupt increases in adsorption at low times before reaching the plateaus. According to these data, equilibrium is achieved at around 120 and 90 min for systems Th^{4+}/SMC-1 and Th^{4+}/SMC-$1_{Zr/SH}$, respectively. However, to ensure the best adsorption conditions at higher concentrations levels, to obtain equilibrium at the solid/liquid interface, all the experiments were conducted within 150 min of contact time. This short time period required to attain equilibrium suggests an excellent affinity of the metal for these phyllosilicates from aqueous solution, principally with the hybrid phyllosilicate. In order to study the specific rate constant of Th^{4+}-phyllosilicate systems, a Lagergren pseudo-second-order rate equation was used to simulate the kinetic adsorption of metals on the phyllosilicates. When the rate of reaction of an adsorption reaction is controlled by chemical exchange, then a pseudo-second order model can be better adjusted to the experimental kinetic data [50], as expressed by Table 3. Conducting a set of experiments at constant temperature and monitoring the amount adsorbed with time, the kinetics of the adsorption process should be known. The rate of metal uptake during the entire period of adsorption was found to be independent of the metal initial concentration used. The correlation coefficient of the pseudo-second-order rate equation (R^2) for the regression non-linear was approximately 0.99, which suggests that the kinetic adsorption can be described by the pseudo-second-order rate equation with satisfactory approximation of experimental kinetic curves.

Based on the second-order model, the initial adsorption rate [51] and half-adsorption time [52] are estimated with the following Eqs. (16) and (17):

$$h = k_2 N_{fEQ}^2 \tag{16}$$

$$t_{\frac{1}{2}} = \frac{1}{k_2 N_{fEQ}} \tag{17}$$

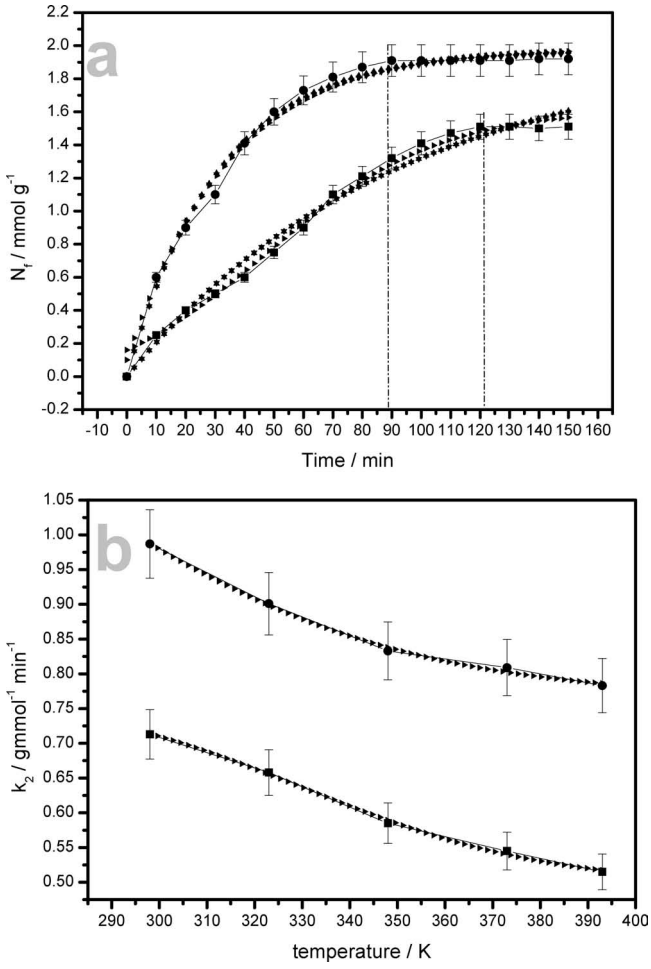

Fig. 6 : Kinetic curves: experimental, SMC-1 ■ and SMC-$1_{Zr/SH}$ •, pseudo-first-order ▼, pseudo-second-order ▲, and Avrami ▶ (a) and activation energy calculated by non-linear of Arrhenius equation ▶ (b) at pH 6.0, after 150 min at 298 – 393 K.

The half-adsorption time $t_{½}$ is another parameter and defined as the time required for the adsorption to take up half as much thorium as its equilibrium values for two systems. Thus, the initial adsorption rate and half-adsorption time are usually a measure of adsorption rate.

Table 3: Isotherms equilibrium and kinetic adsorption parameters (clay 1.0 g dm^{-3}, pH 6.0, time 150 min and temperature of 298 ± 1 K)

Adsorption models	Parameter Values	
	SMC-1	$SMC\text{-}1_{Zr/HS}$
Isotherms equilibrium models		
Langmuir		
N_L (mmol g^{-1})	1.672	2.599
K_L (dm^3 $mmol^{-1}$)	1.173	1.248
R^2 adjusted	0.997	0.989
F_{error}	0.501	0.712
Freundlich		
K_F [mmolg^{-1} (mmoldm^{-3})$^{-1/n_F}$]	0.431	0.664
n_F	1.222	1.012
R^2 adjusted	0.965	0.962
F_{error}	0.898	0.994
Sips		
N_S (mmol g^{-1})	1.564	1.995
K_S (mmoldm^{-3}) $^{-1/n_S}$	1.004	1.002
n_S	0.798	0.871
R^2 adjusted	0.999	0.999
F_{error}	0.216	0.201
Kinetic models		
Avrami		
N_S (mmol g^{-1})	1.556	1.899
k_{AV} (min^{-1})	0.732	0.995
n_{AV}	0.977	0.966
R^2 adjusted	0.998	0.997
F_{error}	0.111	0.112
Pseudo-first-order		
N_S (mmol g^{-1})	1.577	1.887
k_f (min^{-1})	0.705	0.934
R^2 adjusted	0.997	0.996
F_{error}	0.122	0.128
Pseudo-second-order		
N_S (mmol g^{-1})	1.601	1.908
k_s (g $mmol^{-1}min^{-1}$)	0.713	0.987
h(mmol $g^{-1}min^{-1}$)	1.828	3.593
$t_{½}$	0.876	0.531
R^2 adjusted	0.999	0.999
F_{error}	0.102	0.105

For determination of activation energy E_a (kJmol^{-1}) for thorium adsorption reaction, the pseudo-second-order rate constant k_2 was expressed as a function of five different temperatures T (298, 323, 348, 373, and 393 ± 1 K) based on an Arrhenius -relationship (Eq. (18)) [52].

$$k_2 = k_0 - \exp\left(\frac{E_a}{RT}\right) \quad (18)$$

where k_0 is the temperature-independent factor (g mol^{-1} min^{-1}) and R is the gas constant (8.314 J mol^{-1} K^{-1}). From this equation and non-linear method, the rate constant values of adsorption k_0 are 6.782 10^{-3} and 9.031 10^{-3} g mol^{-1} min^{-1} and the activation energy values of adsorption are -25.08 and -28.60 kJ mol^{-1} for SMC-1 and $SMC\text{-}1_{Zr/SH}$, respectively. These values show that thorium adsorption processes with surface clay adsorbents are exothermic. These results may be explained by the fact that the adsorption phenomena are in many systems an exothermic and spontaneous process [52, 53], the values of determination coefficient (R^2) for both calculated curves were approximately 0.999. The pseudo-second-order kinetic constant decreased with increasing temperature (Fig. 6b).

(4) Column thorium adsorption

In order to evaluate natural and modified smectite samples as absorbents for wastewater treatment of Th^{4+} containing effluents, breakthrough time curves of this metallic ion using SMC-1 and $SMC\text{-}1_{Zr/SH}$ as absorbents were obtained, as illustrated in Figs. 7a - 7d. In this work, two initial concentrations were used to evaluate the performance in the glass column system (11.0 and 35.0 x 10^{-2} mg dm^{-3}). Fig. 7a shows the effect of the influent concentrations of Th^{4+} on the shape of breakthrough time curves at the same flow rate (11.0 cm^3 min^{-1}). Specifically, breakthrough time is defined as the time elapsed between initial contact of the metallic solution with the outside surface of the natural and modified silicates and the time at which the metallic ion reaches the number maximum of reactive sites in the silicate surfaces. The results shown in Figs. 7a and 7b indicate that breakthrough time decreases as thorium concentration increases, with the curve showing an S-type model [54 - 56]. The column adsorption capacities N_{ed} for Th^{4+} by natural and modified clay samples are 37.01 and 45.42 mg g^{-1} by SMC-1 and 66.12 and 75.80 mg g^{-1} by $SMC\text{-}1_{Zr/SH}$ when influent concentrations are 10.0 and 30.0 mg dm^{-3}, respectively. The N_{ed} at 30.0 mg dm^{-3} is higher than those at 10.0 mg dm^{-3}; this can be attributed to the concentration gradient, which will enhance the adsorption process [54 - 56].

To investigate the effect of flow rates on the breakthrough curves of Th^{4+} adsorption, 15.0 x 10^{-2} mg dm^{-3} of thorium was fixed as the influent concentration, and the flow rates were 5.0 and 10.0 cm^3 min^{-1}, respectively. The breakthrough curves are shown in Figs. 7c and 7d. The breakthrough curve generally occurs faster with higher flow rate at 10 cm^3 min^{-1}, compared to that of the flow rate at 5.0 cm^3 min^{-1}. The breakthrough time increases with the decrease of flow rate, and therefore, the adsorption of Th^{4+} was given more time to contact with the natural and modified smectite samples at a lower flow rate, which may result in the higher adsorption efficiency of Th^{4+} in

the glass column system [54 - 56]. The results were verified by the N_{ed} at two flow rates (5.0 and 10.0 cm^3 min^{-1}), which are 36.91 and 37.12 mg g^{-1} by SMC-1 and 65.92 and 66.01 mg g^{-1} by SMC-$1_{Zr/SH}$, respectively. Based on the results presented, the effect of the flow rate can be ignored when it is lower than 5.0 cm^3 min^{-1}, in concordance with results reported by Xu *et al.*, 2009 [57], for the adsorption of phosphate from aqueous solution using modified wheat residue (MWS).

IV. Conclusion

The achievement of the pillaring process and the compound 3-mercaptopropyltrimethoxysilane attachment onto a smectite surface and the capacity of this hybrid material to easily adsorb Th^{4+} ions from water have been demonstrated. Adsorption on natural or modified smectite clay samples increased continuously with temperature. The most appropriate condition was pH 6.0 at 298 ± 1 K, to present a plateau at 90 and 120 min, the stabilization time for two matrices was considered of affinity for reaction metal-smectites. The pseudo second-order model provided the best correlation of the experimental data. The uptake of cations was very fast initially for both inorganic supports before reaching the plateau. The Langmuir isotherms yielded good fits with the adsorption data for tetravalent metal/clay interactions ($R^2 \sim 0.99$).

The adsorption results were confirmed through stable complexes formed between cations and free electrons pairs on the sulfur atoms deposited on the pendant groups, whose behavior was checked with the thermodynamic values obtained by means of calorimetry. The quantitative metal/reactive center interactions of modified smectite clay were observed with the calorimetric method at the solid/liquid interface to give favorable sets of data, such as exothermic enthalpy, negative Gibbs free energy, and positive entropic values. These thermodynamic and adsorption values suggest the application of this material, available worldwide, to improve the environment as cation extraction agents.

Acknowledgements

The authors are grateful to MCT, CNPq, and CAPES for financial support and fellowships.

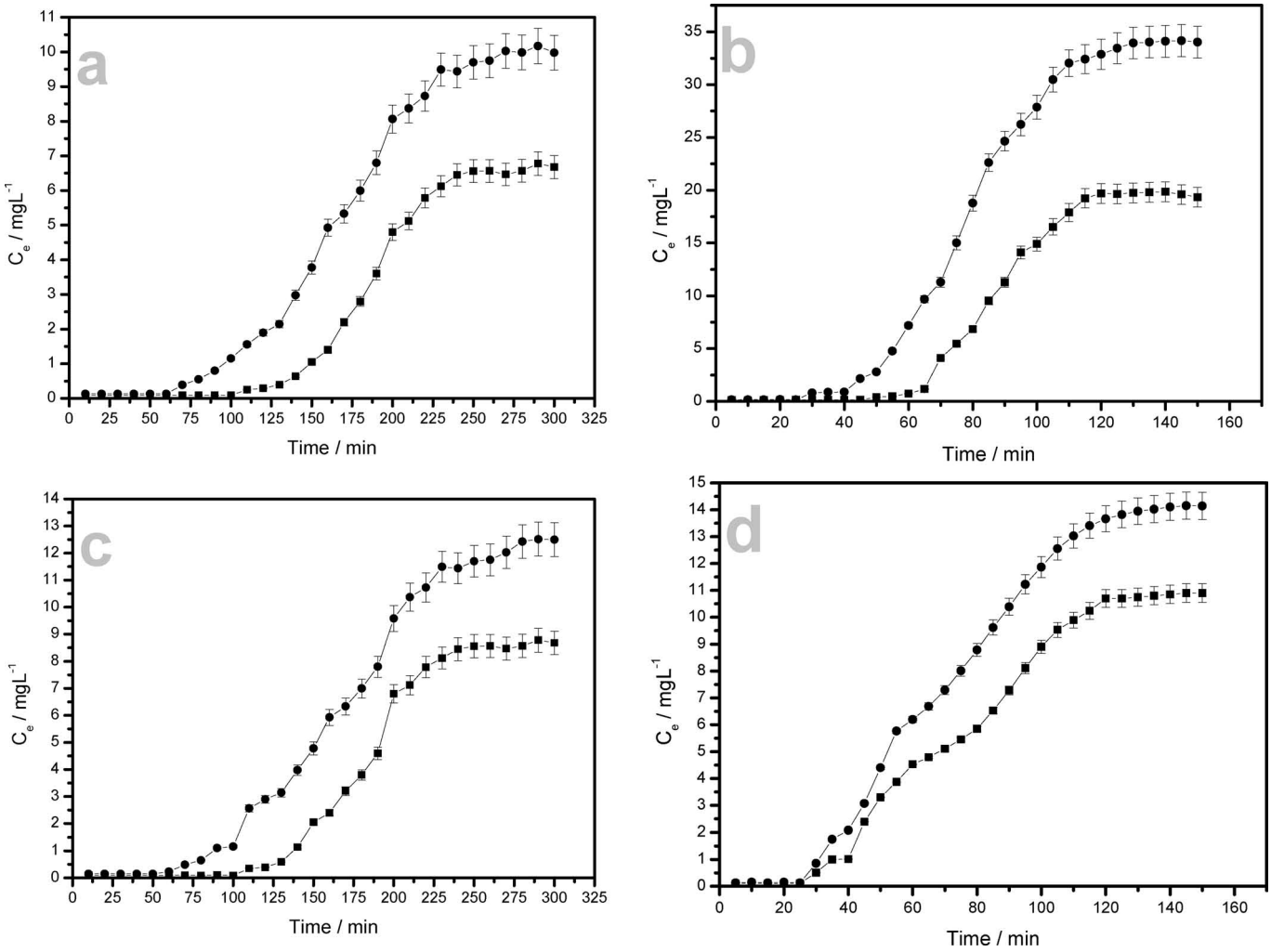

Fig. 7 Effect of variation influent concentration on the breakthrough time curves, SMC-1 ■ and SMC-$1_{Zr/SH}$ •: 11.0 mg dm^{-3} (a) and 35.0 mg dm^{-3} (b) and breakthrough curves of various flow rates 5.0 cm^3 min^{-1}(c) and 10.0 cm^3 min^{-1} (d) at pH 6.0, after 150 and 300 min at 298 ± 1 K.

Nomenclature

N_f the maximum adsorption capacity of the adsorbent (mmol g^{-1})

C_S metal concentration at equilibrium (mmol dm^{-3})

N_L amount of adsorbate adsorbed at the equilibrium-Langmuir (mmol g^{-1})

K_L Langmuir affinity constant (dm^{-3} $mmol^{-1}$)

K_F Freundlich constant related to adsorption capacity [mmol g^{-1}(mmol $dm^{-3})^{-1/n_F}$]

n_F dimensionless exponent of Freundlich equation

N_S amount of adsorbate adsorbed at the equilibrium-Sips (mmol g^{-1})

K_S Sips constant related to the affinity constant [(mmol $dm^{-3})^{-1/n_S}$]

n_S dimensionless exponent of Sips equation

N_t amount of adsorbate adsorbed at time t (mmol g^{-1})

N_E amount of adsorbate adsorbed at the equilibrium-kinetic (mmol g^{-1})

k_{AV} Avrami kinetic constant (min^{-1})

t time of contact (min)

k_f pseudo-first-order rate constant (min^{-1})

k_s pseudo-first-order rate constant (g $mmol^{-1}$ min^{-1})

References

1 Guerra, D.L., Lemos, V.P., Airoldi, C., Angélica, R.S.: Influence of the acid activation of pillared smectites from amazon (Brazil) in adsorption process with butylamine, *Polyhedron*, **25**, 2880 - 2890, (2006).

2 Liou, T.H.: Development of mesoporous structure and high adsorption capacity of biomass based activated carbon by phosphoric acid and zinc chloride activation, *Chem. Eng. J.*, **158**, 129 - 142, (2010).

3 Salinas-Castillo, A., Pastor, I., Mallavia, R., Mateo, C.R.: Immobilization of a trienzymatic system in a sol-gel Matrix: A new fluorescent biosensor for xanthine, *Biosens. Bioelectron.*, **24**, 1053 - 1056, (2008).

4 Caillou, S., Gerin, P.A., Nonckreman, C.J., Fleith, S., Dupont-Gillain, C.C., Landoulsi, J., Pancera, S.M., Genet, M.J., Rouxhet, P.G.: Enzymes at solid Surfaces: nature of the interface and physico-chemical process, *Electrochim. Acta*, **54**, 116 - 122, (2008).

5 Sales, J.A.A., Airoldi, C.: Epoxide silylant agent ethylenediamine reaction product anchored on silica gel - thermodynamics of cation-nitrogen interaction at solid/liquid interface, *J. Non-Cryst. Solids*, **330**, 142 - 149, (2003).

6 Türünç, O., Kahraman, M.V., Akdemir, Z.S., Kayaman-Apohan, N., Güngör, A.: Immobilization of α-amylase onto cyclic carbonate bearing hybrid material, *Food Chem.*, **112**, 992 - 997, (2009).

7 Guerra, D.L., Airoldi, C.: The performance of urea-intercalated and delaminated kaolinite-adsorption kinetics involving copper and lead, *J. Brazil. Chem. Soc.*, **20**, 19 - 30, (2009).

8 Tekin, N., Kadinci, E., Demirbas, Ö., Alkan, M., Kara, A.: Adsorption of polyvinylimidazole onto kaolinite, *J. Colloid Interface Sci.*, **89**, 472 - 479, (2006).

9 Zhao, D.L., Feng, S.J., Chen, C.L., Chen, S.H., Xu, D., Wang, X.K.: Adsorption of Thorium(IV) on MX-80 Bentonite: effect of pH, ionic strength and temperature, *Appl. Clay Sci.*, **41**, 17 - 23, (2008).

10 Degueldre, C., Kline, A.: Study of thorium association and surface precipitation on colloids, *Earth Planet. Sci. Lett.*, 264, 104 - 113, (2007).

11 Manohar, D.M., Noeline, B.F., Anirudhan, T.S.: Adsorption performance of al-pillared bentonite clay for the removal of Cobalt(III) from aqueous phase, *Appl. Clay Sci.*, **31**, 194 - 206, (2006).

12 Karabulut, S., Karabulut, A., Denizli, A., Yürüm, Y.: Batch removal of Copper(II) and Zinc(II) from aqueous solutions with low-rank turkish coals, *Sep. Purif. Technol.*, **18**, 177 - 184, (2000).

13 Babel, S., Kurniawan, T.A.: Cr(VI) removal from synthetic wastewater using coconut shell charcoal and commercial activated carbon modified with oxidizing agents and/or chitosan, *Chemosphere*, **54**, 951 - 967, (2004).

14 Minamisawa, M., Minamisava, H., Yoshida, S., Takai, N.: Adsorption behavior of heavy metals on biomaterials, *J. Agr. Food Chem.*, **52**, 5606 - 5611, (2004).

15 Kanaan, N., Malar, S.J.S.: Removal of mercury (II) ions by adsorption onto dates nut and commercial activated Carbons: A comparative study, *Indian J. Chem. Techn*., **12**, 522 - 527, (2005).

16 Almond, G.G., Harris, R.K., Franklin, K.R.: Sorption Behavior of U(VI) on Phyllite: Experiments and Modeling, *J. Mater. Chem.*, 7, 681 - 687, (1997).

17 Leppert, D.: Heavy Metals Sorption with Clinoptilolite Zeolite: Alternatives for Treating Contaminated Soil and Water, *Min. Engng.*, **42**, 604 - 608, (1990).

18 Tang, X., Li, Z., Chen, Y.: Adsorption behavior of Zn(II) on calcinated chinese loess, *J. Hazard. Mater.*, **161**, 824 - 834, (2009).

19 Xu, S., Boyd, S.A.: Cationic surfactant adsorption by swelling and non-swelling layer silicates, *Langmuir*, **11**, 2508 - 2514, (1995).

20 Penner, D., Lagaly, G.: Influence of Organic and Inorganic Salts on the Coagulation of Montmorillonite Dispersions, *Clay Clay Miner.*, **48**, 246 - 255, (2000).

21 Luptáková, V., Plesch, G.: Intercalated Cu(II) Benzimidazole Complexes in the Interlayer Space of Montmorillonite, *Clay Miner.*, **40**, 295 - 302, (2005).

22 Talip, Z., Eral, M., Hiçsönmez, Ü.: Adsorption of thorium from aqueous solutions by perlite, *J. Environ. Radioactiv.*, **100**, 139 - 143, (2009).

23 Guerra, D.L., Silva, E.M., Lara, W., Batista, A.C.: Removal of Hg(II) from aqueous medium by adsorption onto natural and alkyl-amine modified brazilian bentonite, *Clay. Clay Miner.*, **59**, 568 - 580, (2011).

24 Acharya, J., Sahu, J.N., Mohanty, C.R., Meikap, B.C.: Removal of Lead(II) from wastewater by activated carbon developed from tamarind wood by zinc chloride activation, *Chem. Eng. J.*, **149**, 249 - 262, (2009).

25 Langmuir, I.: The adsorption of gases on plane surfaces of glass, mica and platinum, *J. Am. Chem.*, **57**, 1361 - 1403, (1918).

26 Freundlich, H.M.F.: Über die adsorption in Lösungen (Adsoption in Solution), *Z. Phys. Chem.*, **57**, 385 - 470, (1906).

27 Sips, R.: On the structure of a catalyst surface, *J. Chem. Phys.*, **16**, 490 - 495, (1948).

28 Cestari, A.R., Vieira, E.F.S., Vieira, G.S., da Costa, L.P., Tavares, A.M.G., Loh, W., Airoldi, C.: The removal of reactive dyes from aqueous solutions using chemically modified mesoporous silica in the presence of anionic surfactant – the temperature dependence and a thermodynamic multivariate analysis, *J. Hazard. Mater.*, **161**, 307 - 316, (2009).

[29] Zachara, J.M., McKinley, J.P.: Influence of Hydrolysis on the Sorption of Metal Cations by Smectites: Importance of Edge Coordination Reactions, *Aquat. Sci.*, **55**, 250 - 261, (1993).

[30] Nunes, L.M., Airoldi, C.: Intercalation behaviour of some aromatic heterocyclic amines into α-titanium hydrogen phosphate, *Mater. Res. Bull.*, **34**, 2121 - 2130, (1999).

[31] Nunes, L.M., Airoldi, C.: The intercalation of some heterocyclic amines into α-titanium Hydrogenphosphete-Structural and calorimetric data, *J. Solid State Chem.*, **154**, 557 - 563, (2000).

[32] Prado, A.G.S., Airoldi, C.: Adsorption, preconcentration and separation of cations on silica gel chemically modified with herbicide 2,4-dichlorophenoxyacetic acid, *Anal. Chim. Acta*, **432**, 201 - 211, (2001).

[33] Prado, A.G.S., Arakaki, L.N.H., Airoldi, C.: Adsorption and separation of Cations on silica gel chemically modified by homogeneous and heterogeneous routes with the Ethylenimine anchored on Thiol modified silica gel, *Green Chem.*, **4**, 42 - 46, (2002).

[34] Lima, I.S., Airoldi, C.: A Thermodynamic Investigation on Chitosan-Divalent Interactions, *Thermochim. Acta*, **421**, 133 - 139, (2004).

[35] Ruiz, V.S.O., Airoldi, C.: Thermochemical data for n-alkylmonoamine intercalation into crystalline lamellar zirconium phenylphosphonate, *Thermochim. Acta*, **420**, 73 - 78, (2004).

[36] Herrero, R., Lodeiro, P., Rey-Castro, C., Vilariño, T., Vicente, M.E.S.: Removal of inorganic mercury from aqueous solutions by biomass of the marine macroalga *Cystoseira baccata*, *Water Res.*, **39**, 3199 - 3210, (2005).

[37] Ruiz, V.S.O., Petrucelli, G.C., Airoldi, C.: Inorganic-organic hybrids derived from lamellar acidic kenyiate immobilizations for cation removal at the Solid/Liquid interface, *J. Mater. Chem.*, **16**, 2338 - 2346, (2006).

[38] Guerra, D.L., Viana, R.R., Airoldi, C.: Adsorption of mercury cation on chemical modified clay, *Mater. Res. Bull.*, **44**, 485 - 491, (2009).

[39] Lazarin, A.M., Airoldi, C.: Thermodynamic of the nickel and cobalt removal from aqueous solution by layered crystalline organofunctionalized barium phosphate, *J. Chem. Thermodyn.*, **41**, 21 - 25, (2009).

[40] Guerra, D.L., Viana, R.R., Airoldi, A.: Thermochemical data for n-alkylmonoamine functionalization into lamellar silicate al-kanemite, *J. Chem. Thermodyn.*, **43**, 69 - 74, (2011).

[41] Burnham, A.K., Dinh, L.N.: A comparison of isoconversional and model-fitting approaches to kinetic parameter estimation and application predictions, *J. Therm. Anal. Calorim.*, **89/2**, 479 – 490, (2007).

[42] Girgis, B.S., El-Barawy, K.A., Felix, N.S.: Dehydration kinetics of some Smectite: A thermogravimetric study, *Thermochim. Acta*, **111**, 9 - 19, (1987).

[43] Sales, J.A.A., Faria, F.P., Prado, A.G.S., Airoldi, C.: Attachment of 2-aminomethylpyridine molecule onto grafted silica gel surface and its ability in chelating cations, *Polyhedron*, **23**, 719 - 725, (2004).

[44] Ebrahimi-Kahrizsangi, R., Abbasi, M.H.: Evaluation of the teliability of coats-redfern methods for the kinetic analysis of non-isothermal TGA, *T. Nonferr. Met. Soc.*, **18**, 217 - 221, (2008).

[45] Horovitz, H.H., Metzger, G.: A new analysis of thermogravimetric traces, *Anal. Chem.*, **35**, 1464 – 1468, (1963).

[46] Guo, P., Duan, T., Song, X., Xu, J., Chen, H. : Effect of soil pH and organic matter on distribution of thorium fractions in soil contaminated by rare-earth industries, *Talanta*, 77, 624 - 627, (2008).

[47] Bhainsa, K.C., D'Souza, S.F.: Thorium biosorption by *Aspergillus Fumigatus*, a filamentous fungal biomass, *J. Hazard. Mater.*, **165**, 670 - 676, (2009).

[48] Crespo, M.T., Gascón, J.L., Acena, M.L.: Techniques and analytical methods in the determination of uranium, thorium, plutonium, americium and radium by adsorption on manganese dioxide, *Sci. Total Environ.*, **130 – 131**, 383 - 391, (1993).

[49] Murphy, R.J., Lenhart, J.J., Honeyman, B.D.: The sorption of thorium (IV) and uranium (VI) to hematite in the presence of natural organic matter, *Colloids Surf. A.*, **157**, 47 - 62, (1999).

[50] Pang, X., Tang, F.: Morphological control of mesoporous materials using inexpensive silica sources, *Micropor. Mesopor. Mat.*, **85**, 1 - 6, (2005).

[51] Catalano, J.G., Brown Jr., G.E.: Uranyl Adsorption onto Montmorillonite: Evaluation of Binding Sites and Carbonate Complexation, *Geochim. Cosmochim. Acta*, **12**, 2995 - 3005, (2005).

[52] Yeddou, N., Bensmaili, A.: Kinetic models for the sorption of dye from aqueous solution by clay-wood sawdust mixture, *Desalination*, **185**, 499 - 508, (2005).

[53] Hongxia, Z., Yongxin, X., Zuyi, T.: Sorption of uranyl ions Gibbsite: effects of contact time, pH, ionic strength, concentration and anion of electrolyte, *Colloids Surf. A.*, **252**, 1 - 5, (2005).

[54] Goel, J., Kadirvelu, K., Rajagopal, C., Gary, V.K.: Removal of lead (II) by adsorption using granular activated Carbon: batch and column studies, *J. Hazard. Mater.*, **125**, 211 - 220, (2005).

[55] Han, R.P., Zhang, J.H., Zou, W.H., Xiao, H.J., Shi, J., Liu, H.M.: Biosorption of Copper(II) and Lead(II) from aqueous solution by chaff in a fixed-bed column, *J. Hazard. Mater.*, **133**, 262 - 268, (2006).

[56] Han, R.P., Wang, Y., Zou, W.H., Wang, Y.F., Shi, J.: Comparison of linear and nonlinear analysis in estimating the thomas model parameters for methylene blue adsorption onto natural zeolite in fixed-bed column, *J. Hazard. Mater.*, **145**, 331 - 335, (2007).

[57] Xu, X., Gao, B., Wang, W., Yue, Q., Wang, Y., Ni, S.: Adsorption of phosphate from aqueous solutions onto modified wheat Residue: characteristics, kinetics and column studies, *Colloids Surf. B*, 70, 46 - 52, (2009).